

Synthesis and Characterization of Octa- and Hexanuclear Polyoxomolybdate Wheels: Role of the Inorganic Template and of the Counterion

Anne Dolbecq,^{*,†} Laurent Lisnard,[†] Pierre Mialane,[†] Jérôme Marrot,[†] Marc Bénard,[‡] Marie-Madeleine Rohmer,[‡] and Francis Sécheresse[†]

Institut Lavoisier de Versailles, UMR 8180, Université de Versailles Saint-Quentin en Yvelines, 45 Avenue des Etats-Unis, 78035 Versailles Cedex, France, and Laboratoire de Chimie Quantique, Institut de Chimie, UMR 7177, CNRS/Université Louis Pasteur, 4 rue Blaise Pascal, 67037 Strasbourg Cedex, France

Received March 10, 2006

Eight new compounds based on $[\text{O}_3\text{PCH}_2\text{PO}_3]^{4-}$ ligands and $\{\text{Mo}^{\text{V}}_2\text{O}_4\}$ dimeric units have been synthesized and structurally characterized. Octanuclear wheels encapsulating various guests have been isolated with different counterions. With NH_4^+ , a single wheel was obtained, as expected, with the planar CO_3^{2-} guest, $(\text{NH}_4)_{12}[(\text{Mo}^{\text{V}}_2\text{O}_4)_4(\text{O}_3\text{PCH}_2\text{PO}_3)_4(\text{CO}_3)_2] \cdot 24\text{H}_2\text{O}$ (**1a**), while with the pyramidal SO_3^{2-} guest, only the syn isomer $(\text{NH}_4)_{12}[(\text{Mo}^{\text{V}}_2\text{O}_4)_4(\text{O}_3\text{PCH}_2\text{PO}_3)_4(\text{SO}_3)_2] \cdot 26\text{H}_2\text{O}$ (**2a**) was characterized. The corresponding anti isomer was obtained with Na^+ as counterions, $\text{Na}_{12}[(\text{Mo}^{\text{V}}_2\text{O}_4)_4(\text{O}_3\text{PCH}_2\text{PO}_3)_4(\text{SO}_3)_2] \cdot 39\text{H}_2\text{O}$ (**2b**), and with mixed Na^+ and NH_4^+ counterions, $\text{Na}^+(\text{NH}_4)_{11}[(\text{Mo}^{\text{V}}_2\text{O}_4)_4(\text{O}_3\text{PCH}_2\text{PO}_3)_4(\text{SO}_3)_2] \cdot 13\text{H}_2\text{O}$ (**2d**). With $[\text{O}_3\text{PCH}_2\text{PO}_3]^{4-}$ extra ligands, the octanuclear wheel $\text{Li}_{12}(\text{NH}_4)_2[(\text{Mo}^{\text{V}}_2\text{O}_4)_4(\text{O}_3\text{PCH}_2\text{PO}_3)_4(\text{HO}_3\text{PCH}_2\text{PO}_3)_2] \cdot 31\text{H}_2\text{O}$ (**4a**) was isolated with Li^+ and NH_4^+ counterions and $\text{Li}_{14}[(\text{Mo}^{\text{V}}_2\text{O}_4)_4(\text{O}_3\text{PCH}_2\text{PO}_3)_4(\text{HO}_3\text{PCH}_2\text{PO}_3)_2] \cdot 34\text{H}_2\text{O}$ (**4c**) as a pure Li^+ salt. A new rectangular anion, formed by connecting two Mo^{V} dimers and two Mo^{VI} octahedra via methylenediphosphonate ligands with NH_4^+ as counterions, $(\text{NH}_4)_{10}[(\text{Mo}^{\text{V}}_2\text{O}_4)_2(\text{Mo}^{\text{VI}}\text{O}_3)_2(\text{O}_3\text{PCH}_2\text{PO}_3)_2(\text{HO}_3\text{PCH}_2\text{PO}_3)_2] \cdot 15\text{H}_2\text{O}$ (**3a**), and $\text{Li}_9(\text{NH}_4)_2\text{Cl}[(\text{Mo}^{\text{V}}_2\text{O}_4)_2(\text{Mo}^{\text{VI}}\text{O}_3)_2(\text{O}_3\text{PCH}_2\text{PO}_3)_2(\text{HO}_3\text{PCH}_2\text{PO}_3)_2] \cdot 22\text{H}_2\text{O}$ (**3d**) as a mixed NH_4^+ and Li^+ salt have also been synthesized. The structural characterization of the compounds, combined with a study of their behavior in solution, investigated by ^{31}P NMR, has allowed a discussion on the influence of the counterions on the structure of the anions and their stability. Density functional theory calculations carried out on both isomers of the $[(\text{Mo}^{\text{V}}_2\text{O}_4)_4(\text{O}_3\text{PCH}_2\text{PO}_3)_4(\text{SO}_3)_2]^{12-}$ anion (**2**), either assumed isolated or embedded in a continuum solvent model, suggest that the anti form is favored by ~ 2 kcal mol $^{-1}$. Explicit insertion of two solvated counterions in the molecular cavity reverses this energy difference and reduces it to less than 1 kcal mol $^{-1}$, therefore accounting for the observed structural versatility.

Introduction

Poly(oxometalates) (POMs) continue to attract interest for their potential applications in the field of catalysis, medicine, and material chemistry.¹ Structural types such as the Keggin and Dawson types have been studied extensively.² These POMs are built from the connection of Mo^{VI} or W^{VI} octahedra around a tetrahedral heteroelement. One of the

strategies for the synthesis of new POM frameworks involves the reduction of poly(oxomolybdates) to give either mixed-valence compounds or fully reduced poly(oxomolybdates) containing the $\{\text{Mo}^{\text{V}}_2\text{O}_4\}$ dimeric structural unit. The reduction can be achieved at room temperature by using a reducing agent such as hydrazine. The group of Müller has extensively used this approach for the design of beautiful and complex wheel-shaped nanosized molecular systems.³ On the other hand, since the first results published by Haushalter and Mundi,⁴ hydrothermal conditions with metallic Mo powder as the usual reducing agent have been successful for the

* To whom correspondence should be addressed. E-mail: dolbecq@chimie.uvsq.fr.

[†] Université de Versailles Saint-Quentin en Yvelines.

[‡] CNRS/Université Louis Pasteur.

(1) Special issue on poly(oxometalates): *Chem. Rev.* **1998**, *98*, 1–387.

(2) Pope, M. T. *Heteropoly and isolopoly oxometalates*; Springer-Verlag: Berlin, 1983.

(3) For example, see: Müller, A.; Roy, S. *Coord. Chem. Rev.* **2003**, *153*.

(4) Haushalter, R.; Mundi, L. *Chem. Mater.* **1992**, *4*, 31.

synthesis of a great number of molecular, one-, two-, or three-dimensional reduced compounds.⁵ The most often encountered structural unit in the family of fully reduced phosphate- and organophosphonatemolybdenum(V) compounds isolated by hydrothermal techniques is the hexanuclear anion built from the connection of three $\{\text{Mo}^{\text{V}}_2\text{O}_4\}$ dimeric fragments around a central phosphate or organophosphonate ligand, with three peripheral phosphate⁶ or organophosphonate ligands.⁷ Syntheses under standard bench conditions afford a large structural diversity of almost exclusively molecular Mo^{V} compounds. Working in nonaqueous solvents, Modéc et al. have synthesized numerous Mo^{V} compounds, with organic ligands coordinated to the Mo ions.⁸ Kamenar et al. have functionalized the dimeric fragment by sophisticated organic ligands.⁹ Kabanos et al. have prepared polyoxomolybdenum(V) complexes with carbonate¹⁰ or sulfite ligands.¹¹ In all these complexes, only one type of organic or inorganic ligand is present. Besides, Kortz and Pope have shown that the reaction of $[\text{O}_3\text{PXPO}_3]^{4-}$ ($\text{X} = \text{O}, \text{CH}_2$) ligands with Mo^{VI} ions could afford a diversity of polyoxomolybdates.¹² We have thus recently initiated a study on the acid–base condensation of the dinuclear $[\text{Mo}^{\text{V}}_2\text{O}_4(\text{H}_2\text{O})_6]^{2+}$ oxocation with $[\text{O}_3\text{PCH}_2\text{PO}_3]^{4-}$ in the presence of a templating exogenous ligand (acetate, formate, or carbonate) and described the synthesis of four cyclic Mo^{V} complexes in an aqueous medium.¹³ Additionally, a tetranuclear Mo^{V} complex with methylenediphosphonate ligands, $[\text{Mo}^{\text{V}}_4\text{O}_{10}(\text{O}_3\text{PCH}_2\text{PO}_3)_2]^{4-}$, had been synthesized in CH_3CN by Chang and Zubieta.¹⁴ All five complexes contain a $\{\text{Mo}^{\text{V}}_2\text{O}_4(\text{O}_3\text{PCH}_2\text{PO}_3)\}$ structural unit, but the connecting modes are completely different. In the cyclic compounds,¹³ the Mo^{V} octahedra are edge-sharing and the organophos-

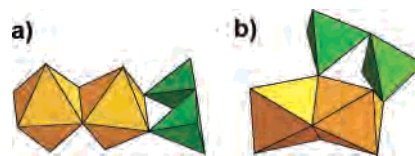


Figure 1. Structure of the $\{\text{Mo}^{\text{V}}_2\text{O}_4(\text{O}_3\text{PCH}_2\text{PO}_3)\}$ unit (a) in the cyclic compounds synthesized in water¹³ and (b) in the tetranuclear complex isolated in CH_3CN .¹⁴ Orange octahedra = MoO_6 . Green tetrahedra = PO_3C .

phonate ligand is connected only to one edge of a Mo^{V} octahedron with Mo–Mo and P–P bonds almost perpendicular (Figure 1a), while in the tetranuclear complex,¹⁴ the Mo^{V} octahedra share one face and the ligand is connected to both Mo^{V} octahedra (Figure 1b). The complexes previously synthesized in an aqueous medium¹³ were all Na^+ salts. We show here how the nature of the counterion in combination with the nature of the exogenous template (carbonate, sulfite, and molybdate) strongly influences the structure of the obtained Mo^{V} complexes. X-ray diffraction studies have been performed to characterize the complexes in the solid state, and their behavior in solution has been thoroughly investigated by ^{31}P NMR, evidencing subtle equilibrium between some species. Density functional theory (DFT) calculations are used to investigate the energy balance between the syn and anti isomers of a hexanuclear wheel and how this balance can be influenced by the nature of the counterions and by the crystal or solvent environment.

Experimental Section

Preparation of a 0.10 M Solution of $[\text{Mo}_2\text{O}_4(\text{H}_2\text{O})_6]^{2+}$ in 4 M HCl. A total of 2.91 g (2.35 mmol) of $(\text{NH}_4)_6\text{Mo}_7\text{O}_{24}\cdot 4\text{H}_2\text{O}$ was dissolved in 80 mL of 4 M HCl, and then 210 μL (4.29 mmol) of $\text{N}_2\text{H}_4\cdot\text{H}_2\text{O}$ was added. The solution turned progressively to red during stirring for 3 h at 60 °C. The solution was then allowed to cool to room temperature. The procedure is identical starting from $\text{Na}_2\text{Mo}^{\text{VI}}\text{O}_4\cdot 2\text{H}_2\text{O}$ (4 g, 16.53 mmol) or $\text{Li}_2\text{Mo}^{\text{VI}}\text{O}_4$ (2.87 g, 16.51 mmol).

Synthesis of $(\text{NH}_4)_{12}[(\text{Mo}^{\text{V}}_2\text{O}_4)_4(\text{O}_3\text{PCH}_2\text{PO}_3)_4(\text{CO}_3)_2]\cdot 24\text{H}_2\text{O}$ (1a). A saturated solution of NH_4HCO_3 was added dropwise until $\text{pH} = 1.5$ to 12.5 mL (1.29 mmol) of a solution of $[\text{Mo}_2\text{O}_4(\text{H}_2\text{O})_6]^{2+}$ obtained from the reduction of $(\text{NH}_4)_6\text{Mo}_7\text{O}_{24}\cdot 4\text{H}_2\text{O}$ as described above. A total of 0.227 g (1.29 mmol) of $\text{H}_4\text{P}_2\text{CH}_2\text{O}_6$ was then added, and the pH was increased to 5.7 by the addition of saturated aqueous ammonium hydrogen carbonate. The solution was then left to evaporate at room temperature. Red parallelepipedic crystals were collected by filtration after 1 week. Yield: 0.33 g (41% based on Mo). FTIR (KBr pellets, cm^{-1}): 1466(s), 1445(s,sh), 1397(s), 1176(s), 1110(sh), 1085(s), 1055(s), 1028(s), 1012(s), 952(s), 916(m,sh), 841(w), 804(m), 747(m), 576(m), 551(m,sh), 482(m). Anal. Calcd for $\text{C}_6\text{H}_{104}\text{Mo}_8\text{N}_{12}\text{O}_{70}\text{P}_8$ (2480.25): C, 2.91; Mo, 30.94; N, 6.78; P, 9.99. Found: C, 3.09; Mo, 31.04; N, 7.17; P, 9.63.

Synthesis of $(\text{NH}_4)_{12}[(\text{Mo}^{\text{V}}_2\text{O}_4)_4(\text{O}_3\text{PCH}_2\text{PO}_3)_4(\text{SO}_3)_2]\cdot 26\text{H}_2\text{O}$ (2a). A total of 1.0 g (7.46 mmol) of $(\text{NH}_4)_2\text{SO}_3\cdot\text{H}_2\text{O}$ was added to 12.5 mL (1.29 mmol) of a solution of $[\text{Mo}_2\text{O}_4(\text{H}_2\text{O})_6]^{2+}$ obtained from the reduction of $(\text{NH}_4)_6\text{Mo}_7\text{O}_{24}\cdot 4\text{H}_2\text{O}$ as described above, and concentrated NH_3 was added dropwise until $\text{pH} = 1.5$. A total of 0.227 g (1.29 mmol) of $\text{H}_4\text{P}_2\text{CH}_2\text{O}_6$ was then added, and the pH was increased to 5.7 by the addition of concentrated NH_3 . After the orange precipitate that had formed was stirred until it dissolved (~ 30 min), the solution was left to evaporate at room temperature.

- (5) For recent examples, see: (a) Khan, M. I.; Chen, Q.; Salta, J.; O'Connor, C.; Zubieta, J. *Inorg. Chem.* **1996**, *35*, 1880. (b) Dumas, E.; Sassoie, C.; Smith, K. D.; Sevov, S. C. *Inorg. Chem.* **2002**, *41*, 4029. (c) du Peloux, C.; Dolbecq, A.; Mialane, P.; Marrot, J.; Rivière, E.; Sécherresse, F. *Angew. Chem., Int. Ed.* **2001**, *40*, 2455. (d) Calin, N.; Sevov, S. C. *Inorg. Chem.* **2003**, *42*, 7304.
- (6) For example, see: (a) Guesdon, A.; Borel, M. M.; Leclair, A.; Raveau, B. *Chem.—Eur. J.* **1997**, *3*, 1797. (b) Xu, L.; Sun, Y.; Wang, E.; Shen, E.; Liu, Z.; Hu, C.; Xing, Y.; Lin, Y.; Jia, H. *J. Solid State Chem.* **1999**, *146*, 533. (c) du Peloux, C.; Mialane, P.; Dolbecq, A.; Marrot, J.; Rivière, E.; Sécherresse, F. *J. Mater. Chem.* **2001**, 3392.
- (7) (a) Cao, G.; Haushalter, R. C.; Strohmaier, K. G. *Inorg. Chem.* **1993**, *32*, 127. (b) Khan, M. I.; Chen, Q.; Zubieta, J. *Inorg. Chim. Acta* **1993**, *206*, 131. (c) Xu, L.; Sun, Y.; Wang, E.; Shen, E.; Liu, Z.; Hu, C.; Xing, Y.; Lin, Y.; Jia, H. *J. Solid State Chem.* **1999**, *146*, 533.
- (8) (a) Modéc, B.; Brencic, J. V.; Zubieta, J. *J. Chem. Soc., Dalton Trans.* **2002**, 1500. (b) Modéc, B.; Brencic, J. V.; Burkholder, E. M.; Zubieta, J. *J. Chem. Soc., Dalton Trans.* **2003**, 4618. (c) Modéc, B.; Brencic, J. V.; Koller, J. *Eur. J. Inorg. Chem.* **2004**, 161.
- (9) (a) Cindric, M.; Vrdoljak, V.; Novak, T. K.; Strukan, N.; Brbot-Saranovic, A.; Novak, P.; Kamenar, B. *Polyhedron* **2004**, *23*, 1859. (b) Cindric, M.; Vrdoljak, V.; Strukan, N.; Tepes, P.; Novak, P.; Brbot-Saranovic, A.; Kamenar, B. *Eur. J. Inorg. Chem.* **2002**, 2128.
- (10) Manos, M. J.; Keramidis, A. D.; Woollins, J. D.; Slawin, A. M. Z.; Kabanos, T. A. *J. Chem. Soc., Dalton Trans.* **2001**, 3419.
- (11) (a) Manos, M. J.; Woollins, J. D.; Slawin, A. M.; Kabanos, T. A. *Angew. Chem., Int. Ed.* **2002**, *41*, 2801. (b) Miras, H. N.; Woollins, J. D.; Slawin, A. M.; Raptis, R.; Baran, P.; Kabanos, T. A. *Dalton Trans.* **2003**, 3668.
- (12) (a) Kortz, U. *Inorg. Chem.* **2000**, *39*, 625. (b) Kortz, U. *Inorg. Chem.* **2000**, *39*, 623. (c) Kortz, U.; Pope, M. T. *Inorg. Chem.* **1995**, *34*, 2160. (d) Kortz, U.; Pope, M. T. *Inorg. Chem.* **1994**, *33*, 5643.
- (13) du Peloux, C.; Dolbecq, A.; Mialane, P.; Marrot, J.; Sécherresse, F. *Dalton Trans.* **2004**, 1259.
- (14) Chang, Y.-D.; Zubieta, J. *Inorg. Chim. Acta* **1996**, *245*, 177.

Red parallelepipedic crystals were collected by filtration after 2 days. Yield: 0.19 g (23% based on Mo). FTIR (KBr pellets, cm^{-1}): 1443(m), 1397(s), 1185(m), 1060(s), 1025(s), 1012(s,sh), 948(m), 902(m), 802(m), 735(w), 557(w), 516(w), 484(w). Anal. Calcd for $\text{C}_4\text{H}_{108}\text{Mo}_8\text{N}_{12}\text{O}_{72}\text{P}_8\text{S}_2$ (2556.39): C, 1.88; Mo, 30.02; N, 6.57; P, 9.69; S, 2.51. Found: C, 1.73; Mo, 29.85; N, 6.55; P, 9.88; S, 2.77.

Synthesis of $(\text{NH}_4)_{10}[(\text{Mo}^{\text{V}}\text{O}_4)_2(\text{Mo}^{\text{VI}}\text{O}_3)_2(\text{O}_3\text{PCH}_2\text{PO}_3)_2\text{-(HO}_3\text{PCH}_2\text{PO}_3)_2]\cdot 15\text{H}_2\text{O}$ (3a**).** A total of 0.114 g (0.092 mmol) of $(\text{NH}_4)_6\text{Mo}_7\text{O}_{24}\cdot 4\text{H}_2\text{O}$ and 0.227 g of (1.29 mmol) of $\text{H}_4\text{P}_2\text{CH}_2\text{O}_6$ were added to 6.25 mL (0.64 mmol) of a solution of $[\text{Mo}_2\text{O}_4(\text{H}_2\text{O})_6]^{2+}$ obtained from the reduction of $(\text{NH}_4)_6\text{Mo}_7\text{O}_{24}\cdot 4\text{H}_2\text{O}$ as described above, and concentrated NH_3 was added dropwise until $\text{pH} = 6.2$. The solution was left to evaporate at room temperature. Red parallelepipedic crystals were collected by filtration after 2 days. Yield: 0.52 g (83% based on Mo). FTIR (KBr pellets, cm^{-1}): 1404(s), 1194(m,sh), 1169(s), 1121(s), 1062(s), 1005(s), 952(s), 904(m), 845(m), 815(s), 742(m), 544(m), 482(m), 448(w). Anal. Calcd for $\text{C}_4\text{H}_{80}\text{Mo}_6\text{N}_{10}\text{O}_{53}\text{P}_8$ (1940.15): C, 2.48; Mo, 29.67; N, 7.22; P, 12.77. Found: C, 2.77; Mo, 29.45; N, 7.65; P, 12.14.

Synthesis of $\text{Li}_{12}(\text{NH}_4)_2[(\text{Mo}^{\text{V}}\text{O}_4)_4(\text{O}_3\text{PCH}_2\text{PO}_3)_4(\text{HO}_3\text{PCH}_2\text{PO}_3)_2]\cdot 31\text{H}_2\text{O}$ (4a**).** A total of 0.39 g (0.19 mmol) of **3d** was dissolved in 8 mL of 4 M LiCl, and the solution was left at room temperature to evaporate. Red crystals were mechanically separated from an orange powder after sonication. Yield: 0.06 g (15% based on Mo). FTIR (KBr pellets, cm^{-1}): 1400(s), 1025(s,sh), 1179(s), 1156(s), 1110(s), 1070(s), 1012(s), 953(s), 919(m), 806(s), 743(w), 628(w), 544(m), 485(m). Anal. Calcd for $\text{C}_6\text{H}_{84}\text{Li}_{12}\text{Mo}_8\text{N}_2\text{O}_{83}\text{P}_{12}$ (2735.20): C, 2.63; H, 3.09; Li, 3.04; Mo, 28.06; N, 1.02; P, 13.59. Found: C, 2.78; H, 2.90; Li, 3.01; Mo, 28.10; N, 1.13; P, 13.39.

Synthesis of $\text{Na}_{12}[(\text{Mo}^{\text{V}}\text{O}_4)_4(\text{O}_3\text{PCH}_2\text{PO}_3)_4(\text{CO}_3)_2]\cdot 72\text{H}_2\text{O}$ (1b**).** **1b** was synthesized as previously described.¹³

Synthesis of $\text{Na}_{12}[(\text{Mo}^{\text{V}}\text{O}_4)_4(\text{O}_3\text{PCH}_2\text{PO}_3)_4(\text{SO}_3)_2]\cdot 39\text{H}_2\text{O}$ (2b**).** A total of 0.5 g (4 mmol) of Na_2SO_3 was added to 6.25 mL (0.64 mmol) of a solution of $[\text{Mo}_2\text{O}_4(\text{H}_2\text{O})_6]^{2+}$ obtained from the reduction of $\text{Na}_2\text{MoO}_4\cdot 2\text{H}_2\text{O}$ as described above and a saturated NaOH solution was added dropwise until $\text{pH} = 1.5$. A total of 0.113 g (0.64 mmol) of $\text{H}_4\text{P}_2\text{CH}_2\text{O}_6$ was then added, and the pH was increased to 5.7 by the addition of a saturated NaOH solution. The solution was left to evaporate at room temperature. Red parallelepipedic crystals were collected by filtration after 2 days. Yield: 0.28 g (61% based on Mo). FTIR (KBr pellets, cm^{-1}): 1369(w), 1184(s), 1117(m), 1066(s), 1027(s), 1008(s,sh), 953(s), 897(m), 849(w), 799(w), 744(w), 553(m), 518(m), 489(m), 407(w), 341(w), 302(w), 280(w). Anal. Calcd for $\text{C}_4\text{H}_{86}\text{Mo}_8\text{Na}_{12}\text{O}_{85}\text{P}_8\text{S}_2$ (2850.00): C, 1.69; Mo, 26.93; Na, 9.68; P, 8.69; S, 2.25. Found: C, 1.93; Mo, 26.51; Na, 10.39; P, 8.74; S, 2.36.

Improved Synthesis of $\text{Na}_8[(\text{Mo}^{\text{V}}\text{O}_4)_3(\text{O}_3\text{PCH}_2\text{PO}_3)_3(\text{Mo}^{\text{VI}}\text{O}_4)]\cdot 18\text{H}_2\text{O}$ (3b**).** The synthesis of **3b** in a 4 M sodium acetate buffer has been previously described.¹³ The yield can be significantly improved by modifying the synthetic procedure. A total of 0.104 g (0.43 mmol) of $\text{Na}_2\text{MoO}_4\cdot 2\text{H}_2\text{O}$ and 0.227 g (1.29 mmol) of $\text{H}_4\text{P}_2\text{CH}_2\text{O}_6$ were added to 12.5 mL (1.29 mmol) of a solution of $[\text{Mo}_2\text{O}_4(\text{H}_2\text{O})_6]^{2+}$ obtained from the reduction of $\text{Na}_2\text{MoO}_4\cdot 2\text{H}_2\text{O}$ as described above, and a saturated NaOH solution was added dropwise until $\text{pH} = 6.0$. The solution was left to evaporate at room temperature. Red parallelepipedic crystals were collected by filtration after 5 days. Yield: 0.40 g (48% based on Mo). FTIR (KBr pellets, cm^{-1}): 1190(s), 1157(s), 1117(m), 1067(s), 1026(s), 949(s), 905(w,sh), 826(w), 798(m), 754(s), 721(m,sh), 553(w), 509(m), 455(w), 393(w), 341(m), 295(w), 260(w). Anal. Calcd for $\text{C}_3\text{H}_{42}\text{Mo}_7\text{Na}_8\text{O}_{52}\text{P}_6$ (1951.68): C, 1.85; H, 2.33; Mo, 34.41; Na^+ , 9.42; P, 9.52. Found: C, 1.91; H, 2.16; Mo, 33.62; Na^+ , 9.44; P, 9.60.

Synthesis of a Solution of $\text{Li}_{12}[(\text{Mo}^{\text{V}}\text{O}_4)_4(\text{O}_3\text{PCH}_2\text{PO}_3)_4\text{-(CO}_3)_2]\cdot n\text{H}_2\text{O}$ (1c**).** A saturated solution of Li_2CO_3 was added dropwise until $\text{pH} = 1.5$ to 12.5 mL (1.29 mmol) of a solution of $[\text{Mo}_2\text{O}_4(\text{H}_2\text{O})_6]^{2+}$ obtained from the reduction of Li_2MoO_4 as described above. A total of 0.227 g (1.29 mmol) of $\text{H}_4\text{P}_2\text{CH}_2\text{O}_6$ was then added, and the pH was increased to 5.7 by the addition of saturated aqueous lithium carbonate. The ^{31}P NMR spectrum of the synthetic solution shows that the major product of the reaction is **1c**. However, no crystals could be obtained by slow evaporation of the solution, probably because of the high solubility of **1c**.

Synthesis of $\text{Li}_8[(\text{Mo}^{\text{V}}\text{O}_4)_3(\text{O}_3\text{PCH}_2\text{PO}_3)_3(\text{Mo}^{\text{VI}}\text{O}_4)]\cdot 19\text{H}_2\text{O}$ (3c**).** A total of 0.074 g (0.43 mmol) of Li_2MoO_4 and 0.227 g (1.29 mmol) of $\text{H}_4\text{P}_2\text{CH}_2\text{O}_6$ were added to 12.5 mL (1.29 mmol) of a solution of $[\text{Mo}_2\text{O}_4(\text{H}_2\text{O})_6]^{2+}$ obtained from the reduction of Li_2MoO_4 as described above, and a saturated LiOH solution was added dropwise until $\text{pH} = 6.0$. The solution was left to evaporate at room temperature. Orange needle crystals were collected by filtration after 5 days. Yield: 0.42 g (53% based on Mo). FTIR (KBr pellets, cm^{-1}): 1192(s), 1152(m), 1123(m,sh), 1077(s), 1030(s), 964(s), 922(w,sh), 812(m), 759(s), 549(s), 512(s,sh), 459(m). Anal. Calcd for $\text{C}_3\text{H}_{44}\text{Li}_8\text{Mo}_7\text{O}_{53}\text{P}_6$ (1841.31): C, 1.95; H, 2.41; Li, 3.01; Mo, 36.47; P, 10.09. Found: C, 2.15; H, 2.50; Li, 3.18; Mo, 32.95; P, 10.26.

Synthesis of $\text{Li}_{14}[(\text{Mo}^{\text{V}}\text{O}_4)_4(\text{O}_3\text{PCH}_2\text{PO}_3)_4(\text{HO}_3\text{PCH}_2\text{PO}_3)_2]\cdot 34\text{H}_2\text{O}$ (4c**).** A saturated LiOH solution was added dropwise to 6.25 mL (0.64 mmol) of a solution of $[\text{Mo}_2\text{O}_4(\text{H}_2\text{O})_6]^{2+}$ obtained from the reduction of Li_2MoO_4 as described above until $\text{pH} = 1.5$. A total of 0.169 g (0.96 mmol) of $\text{H}_4\text{P}_2\text{CH}_2\text{O}_6$ was added, and the pH was adjusted to 3.5 with a saturated LiOH solution. Red parallelepipedic crystals were collected by filtration after 5 days. Yield: 0.22 g (50% based on Mo). FTIR (KBr pellets, cm^{-1}): 1368(w), 1184(s), 1156(s,sh), 1107(s), 1089(s,sh), 1062(s), 1027(s), 1007(s,sh), 960(s), 805(w), 778(w), 741(w), 572(m), 523(m), 486(m). Anal. Calcd for $\text{C}_6\text{H}_{82}\text{Li}_{14}\text{Mo}_8\text{O}_{86}\text{P}_{12}$ (2767.06): C, 2.60; H, 2.98; Li^+ , 3.51; Mo, 27.73; P, 13.43. Found: C, 2.62; H, 2.62; Li^+ , 3.45; Mo, 27.64; P, 13.78.

Synthesis of $\text{Na}(\text{NH}_4)_{11}[(\text{Mo}^{\text{V}}\text{O}_4)_4(\text{O}_3\text{PCH}_2\text{PO}_3)_4(\text{SO}_3)_2]\cdot 13\text{H}_2\text{O}$ (2d**).** A total of 0.460 g of **2b** was dissolved in 7.6 mL of 1 M $(\text{NH}_4)_2\text{SO}_3$ adjusted to $\text{pH} = 5.7$. Red parallelepipedic crystals were collected after 5 days. Yield: 0.36 g (80% based on Mo). The FTIR spectrum is similar to that of **2b**. Anal. Calcd for $\text{C}_4\text{H}_{78}\text{Mo}_8\text{N}_{11}\text{NaO}_{59}\text{P}_8\text{S}_2$ (2327.14): C, 2.06; H, 3.38; Mo, 32.98; N, 6.62; Na, 0.99; P, 10.64. Found: C, 2.01; H, 3.56; Mo, 33.02; N, 6.77; Na, 1.18; P, 9.85.

Synthesis of $\text{Li}_9(\text{NH}_4)_2\text{Cl}[(\text{Mo}^{\text{V}}\text{O}_4)_2(\text{Mo}^{\text{VI}}\text{O}_3)_2(\text{O}_3\text{PCH}_2\text{PO}_3)_2\text{-(HO}_3\text{PCH}_2\text{PO}_3)_2]\cdot 22\text{H}_2\text{O}$ (3d**).** A total of 0.6 g (0.31 mmol) of **3a** was dissolved in 9 mL of 4 M LiCl, and the solution was left to evaporate at room temperature. Red crystals were collected after 2 days. Yield: 0.44 g (69% based on Mo). FTIR (KBr pellets, cm^{-1}): 1397(s), 1207(m,sh), 1178(s), 1156(s,sh), 1111(m), 1067(s), 1014(s), 951(m), 918(w), 856(w), 812(s), 741(w), 546(m), 483(m), 397(w). Anal. Calcd for $\text{C}_4\text{H}_{62}\text{ClLi}_9\text{Mo}_6\text{N}_2\text{O}_{60}\text{P}_8$ (2019.87): C, 2.38; H, 3.09; Cl, 1.75; Li, 3.09; Mo, 28.50; N, 1.39; P, 12.27. Found: C, 2.25; H, 2.76; Cl, 2.00; Li, 3.00; Mo, 28.11; N, 1.47; P, 12.03.

X-ray Crystallography. Intensity data collection was carried out with a Siemens SMART three-circle diffractometer for all of the structures except for **2a**, for which the data were collected with a Bruker Nonius X8 APEX 2 diffractometer, each equipped with a CCD two-dimensional detector using the monochromatized wavelength $\lambda(\text{Mo K}\alpha) = 0.71073 \text{ \AA}$. The absorption correction was based on multiple and symmetry-equivalent reflections in the data set using the *SADABS* program¹⁵ based on the method of Blessing.¹⁶ The structures were solved by direct methods and refined

by full-matrix least squares using the *SHELX-TL* package.¹⁷ In all of the structures, there is a discrepancy between the formulas determined by elemental analysis and the formulas deduced from the crystallographic atom list because of the difficulty in locating all of the disordered water molecules and alkali counterions. Disordered water molecules and alkali counterions have been refined with partial occupancy factors and with isotropic thermal parameters. In the structures of **2a**, **3a**, and **2d**, NH₄⁺ and H₂O could not be distinguished according to the observed electron densities; therefore, all of the positions were labeled O and assigned the oxygen atomic diffusion factor. It has been possible to distinguish the NH₄⁺ ion only in the structures of **4a** and **3d** because of the presence of four H atoms located nearby the N position. Crystallographic data are given in Table 1. Selected bond distances are listed in Table 2. CIF files are given in the Supporting Information.

NMR Measurements. ³¹P NMR spectra were recorded on a Brüker AC-300 spectrometer operating at 121.5 MHz in 5-mm tubes with ¹H NMR decoupling. ³¹P NMR chemical shifts were referenced to the usual external standard of 85% H₃PO₄.

Elemental Analysis. Elemental analyses were performed by the Service Central d'Analyse Élémentaire, CNRS, 69390 Vernaison, France.

IR Spectra. IR spectra were recorded on a Nicolet IRFT Magna 550 spectrophotometer using the technique of pressed KBr pellets.

DFT Calculations. Calculations on [(Mo^V₂O₄)₄(O₃PCH₂PO₃)₄-(SO₃)₂]¹²⁻ (**2**) have been carried out with the ADF program system.¹⁸ The exchange-correlation functional is the so-called Becke–Perdew/86 (BP86) functional.¹⁹ The atomic basis sets used for nonmetal atoms are triple- ζ -quality for the valence shells, supplemented with one polarization function (p type for H atoms and d type for other atoms). The valence shell of Mo (4s/4p/4d/5s) is also triple- ζ , supplemented with one p-type orbital describing the 5p shell. These basis sets have been used in conjunction with frozen cores described with one Slater orbital for each atomic shell and with the zero-order regular approximation (ZORA)²⁰ to the relativistic effects. Basis sets of similar quality have been used to model the Na⁺ and NH₄⁺ counterions in the [Na₂(Mo₂O₄)₄-(O₃PCH₂PO₃)₄(SO₃)₂]¹⁰⁻ and [(NH₄)₂(Mo₂O₄)₄(O₃PCH₂PO₃)₄-(SO₃)₂]¹⁰⁻ host–guest complexes, respectively. The effect of solvation was estimated by means of the COSMO continuum model,²¹ using the dielectric constant of water.

(15) Sheldrick, G. M. *SADABS, program for scaling and correction of area detector data*; University of Göttingen: Göttingen, Germany, 1997.

(16) Blessing, R. *Acta Crystallogr.* **1995**, *A51*, 33.

(17) Sheldrick, G. M. *SHELX-TL*, version 5.03; Software Package for the Crystal Structure Determination; Siemens Analytical X-ray Instrument Division: Madison, WI, 1994.

(18) Baerends, E. J.; Autschbach, J.; Bérces, A.; Bo, C.; Boerrigter, P. M.; Cavallo, L.; Chong, D. P.; Deng, L.; Dickson, R. M.; Ellis, D. E.; Fan, L.; Fischer, T. H.; Fonseca Guerra, C.; van Gisbergen, S. J. A.; Groeneveld, J. A.; Gritsenko, O. V.; Grüning, M.; Harris, F. E.; van den Hoek, P.; Jacobsen, H.; van Kessel, G.; Kootstra, F.; van Lenthe, E.; McCormack, D. A.; Osinga, V. P.; Patchkovskii, S.; Philipsen, P. H. T.; Post, D.; Pye, C. C.; Ravenek, W.; Ros, P.; Schipper, P. R. T.; Schreckenbach, G.; Snijders, J. G.; Sola, M.; Swart, M.; Swerhone, D.; te Velde, G.; Vernooijs, P.; Versluis, L.; Visser, O.; van Wezenbeek, E.; Wiesenekker, G.; Wolff, S. K.; Woo, T. K.; Ziegler, T. ADF2004.01; SCM, Theoretical Chemistry, Vrije Universiteit: Amsterdam, The Netherlands, 2004; <http://www.scm.com>.

(19) (a) Becke, A. D. *Phys. Rev.* **1988**, *A38*, 3098. (b) Perdew, J. P. *Phys. Rev.* **1986**, *B33*, 8822; **1986**, *B34*, 7406.

(20) (a) van Lenthe, E.; Baerends, E.-J.; Snijders, J. J. *Chem. Phys.* **1993**, *99*, 4597. (b) van Lenthe, E.; Baerends, E.-J.; Snijders, J. J. *Chem. Phys.* **1996**, *105*, 6505.

(21) (a) Klamt, A.; Schüürmann, G. *J. Chem. Soc., Perkin Trans.* **1993**, *2*, 799. (b) Klamt, A. *J. Phys. Chem.* **1995**, *99*, 2224. (c) Klamt, A.; Jonas, V. *J. Chem. Phys.* **1996**, *105*, 9972.

Table 1. Crystallographic Data for **1a–4a**, **2b**, **4c**, **2d**, and **3d**

	1a	2a	3a	4a	2b	4c	2d	3d
empirical formula	C ₆ H ₁₀₄ Mo ₈ N ₁₂ O ₇₀ P ₈	C ₄ H ₁₀₈ Mo ₈ N ₁₂ O ₇₂ P ₈ S ₂	C ₄ H ₈₀ Mo ₆ N ₁₀ O ₅₃ P ₈	C ₆ H ₈₄ Li ₁₂ Mo ₈ N ₂ O ₈₃ P ₈ S ₂	C ₄ H ₈₆ Mo ₈ N ₁₂ O ₈₃ P ₈ S ₂	C ₆ H ₈₂ Li ₁₄ Mo ₈ O ₈₆ P ₁₂	C ₇ H ₇₈ Mo ₈ N ₁₁ NaO ₈₉ P ₈ S ₂	C ₄ H ₆₂ ClLi ₉ Mo ₆ N ₂ O ₆₂ P ₈
fw, g	2480.29	2556.39	1972.18	2735.19	2850.00	2767.04	2327.14	2051.87
cryst syst	monoclinic	triclinic	triclinic	monoclinic	triclinic	triclinic	triclinic	triclinic
space group	P2 ₁ /c	P1	P1	P2 ₁ /n	P1	P1	P1	P1
a/Å	16.464(8)	14.439(1)	13.4897(2)	13.422(3)	11.6173(5)	11.8591(1)	9.6783(2)	13.7096(2)
b/Å	13.222(7)	16.333(1)	13.7119(2)	16.329(1)	13.3978(6)	12.9812(1)	14.2098(2)	14.2642(2)
c/Å	17.357(12)	16.610(1)	17.9603(1)	18.598(2)	13.6621(6)	16.0452(1)	14.3744(2)	17.4993(3)
α /deg	90	82.917(3)	73.936(1)	90	75.507(1)	101.200(1)	95.289(1)	101.401(1)
β /deg	114.51(2)	88.179(3)	77.086(1)	102.214(11)	72.349(1)	107.477(1)	95.533(1)	104.101(1)
γ /deg	90	79.074(3)	64.900(1)	90	85.182(1)	108.067(1)	96.213(1)	108.799(1)
V/Å ³	3438(3)	3816.7(4)	2869.36(6)	3983.7(10)	1961.79(15)	1960.72(3)	1945.55(6)	2996.41(8)
Z	2	2	2	2	1	1	1	2
ρ_{calc} /g cm ⁻³	2.396	2.225	2.283	2.280	2.412	2.310	2.221	2.274
μ /mm ⁻¹	1.741	1.626	1.628	1.597	1.662	1.602	1.608	1.610
data/param	4960/433	17414/962	8166/703	5728/563	5628/513	9767/553	9627/436	14721/817
R _{int}	0.0714	0.0541	0.0541	0.0288	0.0293	0.0244	0.0322	0.0336
GOF	1.027	1.131	1.154	0.948	1.073	1.103	1.086	1.068
R [I > 2 σ (I)]	0.0689	0.0528	0.0768	0.0453	0.0433	0.0528	0.0755	0.0614
wR2 ^b	0.1739	0.1564	0.1983	0.1342	0.1039	0.1359	0.1902	0.1543

$$^a R1 = \sum |F_o| - |F_c| / \sum |F_o|, \quad ^b wR2 = \sqrt{\sum w(F_o^2 - F_c^2)^2 / \sum w(F_o^2)}$$

Table 2. Selected Bond Lengths (Å) for 1a–4a, 2b, 4c, 2d, and 3d

	1a	2a	3a	4a	2b	4c	2d	3d
Mo ^V =O	1.672(8)–1.690(7) [1.683]	1.676(4)–1.695(4) [1.686]	1.670(12)–1.716(11) [1.690]	1.672(5)–1.692(5) [1.682]	1.671(5)–1.697(5) [1.680]	1.678(4)–1.700(4) [1.689]	1.671(7)–1.683(7) [1.677]	1.686(5)–1.704(5) [1.693]
Mo ^V –O _{Mo}	1.930(7)–1.957(7) [1.940]	1.937(4)–1.965(4) [1.949]	1.925(11)–1.951(10) [1.939]	1.929(5)–1.953(5) [1.939]	1.922(5)–1.944(5) [1.936]	1.945(4)–1.964(4) [1.953]	1.929(6)–1.951(7) [1.938]	1.936(5)–1.958(5) [1.949]
Mo ^V –O _p	2.066(7)–2.103(7) [2.089]	2.053(4)–2.113(4) [2.095]	2.096(11)–2.150(11) [2.115]	2.052(5)–2.109(5) [2.085]	2.068(5)–2.110(5) [2.084]	2.068(4)–2.137(4) [2.103]	2.068(4)–2.137(4) [2.077]	2.103(5)–2.140(5) [2.117]
Mo ^V –O ^a	2.220(7)–2.509(8) [2.356]	2.202(4)–2.545(4) [2.336]	2.221(10)–2.251(11) [2.234]	2.260(5)–2.505(5) [2.341]	2.266(5)–2.523(5) [2.368]	2.231(4)–2.516(4) [2.367]	2.235(6)–2.490(6) [2.354]	2.193(5)–2.239(5) [2.212]
Mo ^V =O	-	-	1.702(10)–1.716(11) [1.709]	-	-	-	-	1.710(5)–1.711(5) [1.710]
Mo ^{VI} –O _{Mo}	-	-	1.756(10)–1.777(10) [1.766]	-	-	-	-	1.758(5)–1.793(5) [1.774]
Mo ^{VI} –O _p	-	-	2.127(11)–2.243(10) [2.185]	-	-	-	-	2.133(5)–2.255(5) [2.191]
Mo ^V –Mo ^V	2.553(2)–2.554(2) [2.553]	2.568(1)–2.579(1) [2.573]	2.571(2)–2.582(2) [2.576]	2.563(1)–2.568(1) [2.566]	2.555(1)–2.569(1) [2.562]	2.575(1)–2.576(1) [2.575]	2.555(1)–2.566(1) [2.561]	2.576(1)–2.580(1) [2.578]
P=O	1.480(8)–1.510(8) [1.494]	1.506(5)–1.520(4) [1.513]	1.493(12)–1.520(11) [1.504]	1.491(6)–1.503(5) [1.497]	1.485(6)–1.541(5) [1.498]	1.499(4)–1.511(5) [1.505]	1.480(7)–1.502(7) [1.494]	1.497(5)–1.529(5) [1.511]
P–O _H bond valence ^b	-	-	1.550(13), 1.551(13) 1.16, 1.15	1.582(6) 1.06	-	1.595(5) 1.02	-	1.559(6), 1.566(6) 1.13, 1.11
P–O _{Mo}	1.530(7)–1.551(7) [1.538]	1.530(4)–1.553(4) [1.542]	1.505(12)–1.551(13) [1.535]	1.533(5)–1.549(5) [1.538]	1.535(5)–1.556(5) [1.544]	1.539(4)–1.557(4) [1.547]	1.514(7)–1.544(7) [1.533]	1.518(6)–1.547(5) [1.540]
P–C	1.78(1)–1.81(1) [1.80]	1.787(6)–1.814(6) [1.802]	1.756(17)–1.855(16) [1.808]	1.785(8)–1.810(7) [1.800]	1.789(8)–1.802(7) [1.796]	1.799(6)–1.806(5) [1.805]	1.772(10)–1.794(10) [1.782]	1.790(7)–1.817(7) [1.805]
N ₁ encapsulated–O	-	-	-	1.940(12)–2.002(13) [1.986]	2.360(6)–2.717(6) [2.454]	-	2.302(13)–2.605(11) [2.412]	-
Li ₁ encapsulated–O	-	-	-	-	-	1.942(11)–2.091(12) [2.012]	-	-

^a Mo–O bond trans to the Mo=O bond. ^b Bond valence summations²² for the O atom of the P–OH bond.

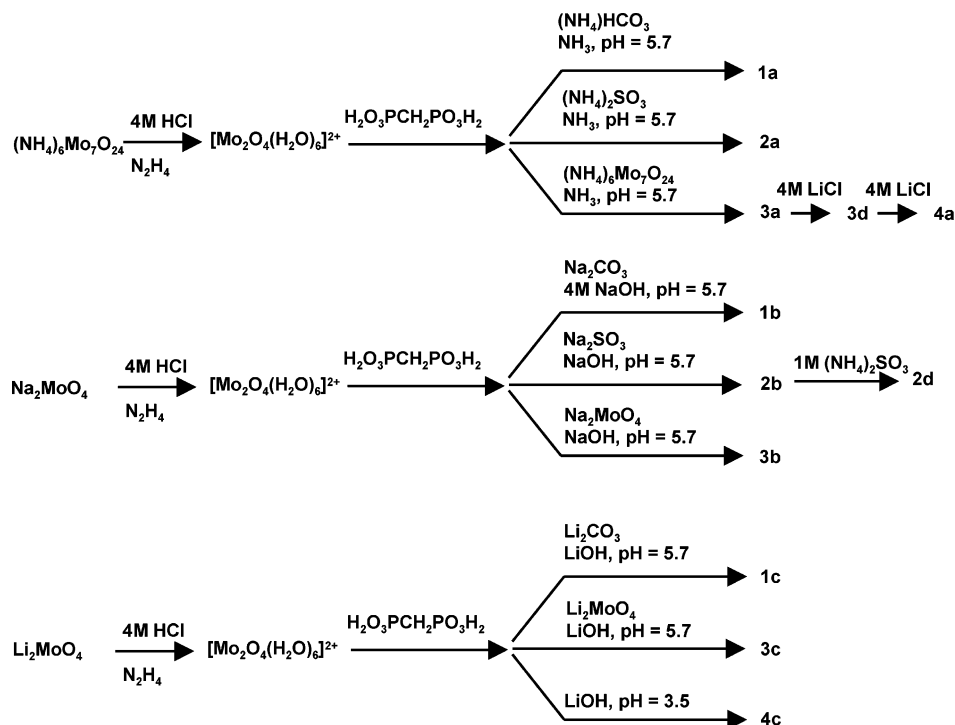


Figure 2. Synthetic routes to compounds 1–4.

Results and Discussions

Synthesis. To systematically study the influence of the counterion on the nature of the Mo^{V} compounds, we have adopted the following synthetic protocol: a solution of the $[\text{Mo}_2\text{O}_4(\text{H}_2\text{O})_6]^{2+}$ cation is obtained by reduction by hydrazine of an acidic solution of the molybdate precursor, $(\text{NH}_4)_6\text{Mo}^{\text{VI}}\text{O}_{24}$, $\text{Na}_2\text{Mo}^{\text{VI}}\text{O}_4$, or $\text{Li}_2\text{Mo}^{\text{VI}}\text{O}_4$. After the pH is raised to 1.5 with NH_3 , NaOH , or LiOH , respectively, the methylenediphosphonic ligand is added. The additional template (CO_3^{2-} , SO_3^{2-} , MoO_4^{2-}) is then added as an NH_4^+ , Na^+ , or Li^+ salt, and the pH rose to 5.7. The synthetic conditions used to obtain 1–4 are summarized in Figure 2. It has been possible to isolate crystals of the NH_4^+ salt, $(\text{NH}_4)_{12}[(\text{Mo}^{\text{V}}_2\text{O}_4)_4(\text{O}_3\text{PCH}_2\text{PO}_3)_4(\text{CO}_3)_2] \cdot 24\text{H}_2\text{O}$ (**1a**), analogous to the Na^+ salt, $\text{Na}_{12}[(\text{Mo}^{\text{V}}_2\text{O}_4)_4(\text{O}_3\text{PCH}_2\text{PO}_3)_4(\text{CO}_3)_2] \cdot 72\text{H}_2\text{O}$ (**1b**).¹³ The analogous Li^+ salt (**1c**) has only been characterized in solution by ^{31}P NMR. With sulfite as the template, two different octanuclear isomers have been isolated, the syn isomer $(\text{NH}_4)_{12}[(\text{Mo}^{\text{V}}_2\text{O}_4)_4(\text{O}_3\text{PCH}_2\text{PO}_3)_4(\text{SO}_3)_2] \cdot 26\text{H}_2\text{O}$ (**2a**) with NH_4^+ as the counterions and the anti isomer $\text{Na}_{12}[(\text{Mo}^{\text{V}}_2\text{O}_4)_4(\text{O}_3\text{PCH}_2\text{PO}_3)_4(\text{SO}_3)_2] \cdot 39\text{H}_2\text{O}$ (**2b**) with Na^+ as the counterions. Despite numerous efforts, we have not been able to isolate or characterize in solution the reaction product with Li^+ counterions. To study the influence of the cation on the stability of the anti isomer, **2b** has been recrystallized in a solution of ammonium sulfite. A mixed NH_4^+ and Na^+ salt $\text{Na}(\text{NH}_4)_{11}[(\text{Mo}^{\text{V}}_2\text{O}_4)_4(\text{O}_3\text{PCH}_2\text{PO}_3)_4(\text{SO}_3)_2] \cdot 13\text{H}_2\text{O}$ (**2d**) is isolated and, surprisingly, the X-ray structure determination (see below) has shown that the presence of one Na^+ ion is sufficient to stabilize the syn isomer. When MoO_4^{2-} ions are added in the synthetic medium, two different anions are isolated: a rectangular anion formed by the connection of two Mo^{V} dimers and two

Mo^{VI} octahedra by methylenediphosphonate ligands with NH_4^+ as the counterions, $(\text{NH}_4)_{10}[(\text{Mo}^{\text{V}}_2\text{O}_4)_2(\text{Mo}^{\text{VI}}\text{O}_4)_2(\text{O}_3\text{PCH}_2\text{PO}_3)_2(\text{HO}_3\text{PCH}_2\text{PO}_3)_2] \cdot 15\text{H}_2\text{O}$ (**3a**), and the previously characterized hexanuclear wheel¹³ with a central $\{\text{Mo}^{\text{VI}}\text{O}_4\}$ tetrahedron, $\text{Na}_8[(\text{Mo}^{\text{V}}_2\text{O}_4)_3(\text{O}_3\text{PCH}_2\text{PO}_3)_3(\text{Mo}^{\text{VI}}\text{O}_4)] \cdot 18\text{H}_2\text{O}$ (**3b**) and $\text{Li}_8[(\text{Mo}^{\text{V}}_2\text{O}_4)_3(\text{O}_3\text{PCH}_2\text{PO}_3)_3(\text{Mo}^{\text{VI}}\text{O}_4)] \cdot 19\text{H}_2\text{O}$ (**3c**) with respectively Na^+ and Li^+ counterions. Finally a new species has been evidenced by the recrystallization of **3a** in LiCl . While the first recrystallization affords a mixed NH_4^+ and Li^+ salt, $\text{Li}_9(\text{NH}_4)_2\text{Cl}[(\text{Mo}^{\text{V}}_2\text{O}_4)_2(\text{Mo}^{\text{VI}}\text{O}_4)_2(\text{O}_3\text{PCH}_2\text{PO}_3)_2(\text{HO}_3\text{PCH}_2\text{PO}_3)_2] \cdot 22\text{H}_2\text{O}$ (**3d**), of the rectangular anion, the second recrystallization has allowed isolation of a new octanuclear anion, with methylenediphosphonate ligands encapsulated within the wheel, $\text{Li}_{12}(\text{NH}_4)_2[(\text{Mo}^{\text{V}}_2\text{O}_4)_4(\text{O}_3\text{PCH}_2\text{PO}_3)_4(\text{HO}_3\text{PCH}_2\text{PO}_3)_2] \cdot 31\text{H}_2\text{O}$ (**4a**). A pure Li^+ salt, $\text{Li}_{14}[(\text{Mo}^{\text{V}}_2\text{O}_4)_4(\text{O}_3\text{PCH}_2\text{PO}_3)_4(\text{HO}_3\text{PCH}_2\text{PO}_3)_2] \cdot 34\text{H}_2\text{O}$ (**4c**), of this new anion has been synthesized in good yield by the addition of a stoichiometric amount of methylenediphosphonic acid to a solution of the oxocation obtained by reduction of lithium molybdate. All of these compounds have been studied in solution by ^{31}P NMR spectroscopy, and the salts have been characterized in the solid state by single-crystal X-ray diffraction, except **1c**, for which it was not possible to isolate a solid, and **3c**, which does not afford single crystals of sufficient quality.

Crystal Structure. A common structural feature of the anions in 1–4 is the presence of $\{(\text{Mo}^{\text{V}}_2\text{O}_4)(\text{O}_3\text{PCH}_2\text{PO}_3)\}$ (Figure 1a) as building units, connected around the templating ligand to form cyclic compounds. The bond distances within the wheel are in the usual range (Table 2).

The anions in **1a** and **1b** are very similar (Figure 3) and can be described as octanuclear ellipsoidal wheels built up of four Mo^{V} dimers connected by methylenediphosphonate

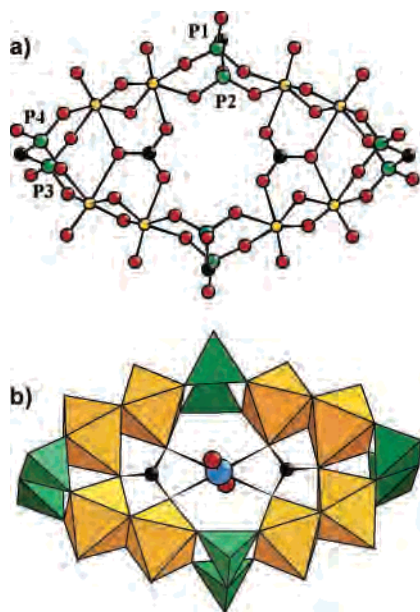


Figure 3. (a) Ball-and-stick representation of the anion in **1a** (orange sphere = Mo, red sphere = O, green sphere = P, and black sphere = C). (b) Polyhedral representation of the anion in **1b** with one Na⁺ ion encapsulated in the wheel (orange octahedra = MoO₆, green tetrahedra = PO₃C, and blue sphere = Na).

ligands. Two μ_4 -CO₃²⁻ ions are encapsulated within the wheel and are located in the plane defined by the Mo^V ions. A μ_2 -O atom of the carbonate ligand ensures the connection of two dinuclear Mo^V units. Both anions have pseudo *D*_{2h} symmetry. The only difference between **1a** and **1b** is that the center of the cavity of the octanuclear wheel in **1b** is occupied by an octahedrally coordinated Na⁺ ion (Table 2) while the cavity in **1a** is empty. ³¹P NMR experiments (see below) have shown that the same wheel is formed in solution with Li⁺ counterions. Therefore, the role of the Na⁺ ion in the formation of the octanuclear wheel in **1b** is probably insignificant, and the carbonate ion plays the major role in structuring the octanuclear wheel.

The inorganic skeleton of the octanuclear wheels in **2a**, **2b**, and **2d** is similar to the one of carbonate wheels, but the templating agents inside the wheel are two pyramidal sulfite ions instead of a planar carbonate ligand (Figure 4). In **2a**, the two sulfite ions are related by a mirror plane and are located on the same side of the plane defined by the eight Mo^V ions, while in **2b** and **2d**, the two S atoms of the sulfite groups are related by an inversion center and lie on two opposite sides of the molecular plane. Therefore, the anion in **2a** is called the syn isomer and the anion common in **2b** and **2d** the anti isomer. In terms of molecular symmetry, the octanuclear wheel in **2a** has *C*_s symmetry and that in **2b** and **2d** *C*_{2h} symmetry. Elemental analysis has shown that **2d** contains only one Na⁺ ion among the 12 counterions. This Na⁺ ion has been located by X-ray diffraction; it is disordered over two positions, related by an inversion center inside the cavity of the wheel (Figure 4b). The Na⁺ ion is bound to two O atoms, which ensure the connection between the methylenediphosphonato group and the Mo^V dimers and to one O atom of each sulfite ligand (Table 2). The coordination sphere is completed by two water molecules,

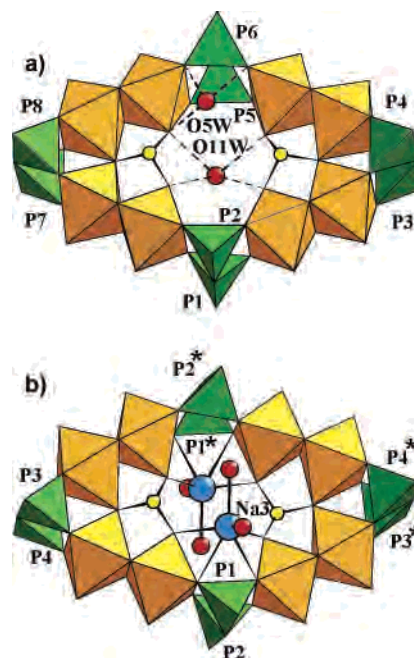


Figure 4. (a) Polyhedral representation of the anion in **2a** showing the syn position of the sulfite groups (orange octahedra = MoO₆, green tetrahedra = PO₃C, and yellow sphere = S). (b) Polyhedral representation of the anion common in **2b** and **2d** showing the anti position of the sulfite groups and the position of the Na⁺ ions coordinated to the two anti sulfite groups; in **2b**, the two Na⁺ ions have full occupancy factors, while in **2d**, they have half-occupancy factors. The stars refer to symmetry-equivalent positions.

one being equally disordered over two positions. In the pure Na⁺ salt (**2b**), the two positions of the Na⁺ cation inside the wheels have full occupancy factors. Therefore, in contrast with the carbonate wheels, the presence of the Na⁺ ion inside the cavity seems to have a crucial role, in the solid state, stabilizing the anti isomer.

The anions in **3a** and **3d** have the same geometrical characteristics (Table 2). The larger sides of the rectangular ion (Figure 5a) are made of a Mo^V dimer, and the smaller sides of a Mo^{VI} octahedron. The corners are occupied by methylenediphosphonato ligands. This anion contains a pseudo mirror plane that intersects the two Mo^V dimers and thus has *C*_s symmetry. However, the asymmetric unit is constituted of a whole anion. There are two different kinds of methylenediphosphonato ligands: in the first one, two O atoms of each phosphonato group (labeled P1, P3, P6, and P8) are bound identically to Mo^V and Mo^{VI} ions, while in the second one, only one phosphonato group (P2 and P5) has two O atoms involved in the connection between a Mo^{VI} octahedron and a Mo^V dimer and the other phosphonato group (P4 and P7) establishes only one bond with a Mo^V dimer, with the other P–O bond pending. Valence bond calculations²² indicate that the O atom of this bond is protonated (Table 2). In **3d**, the H atoms on the P–OH groups (H36 and H38) have been located in the Fourier difference map. They establish H bond interactions with the O atoms of the neighboring phosphate group (O28 and O9, respectively; Figure 5a). The O36–H36···O28 interaction is stronger [H36···O28 = 1.66(1) Å; O36–H36···O28 =

(22) Bresa, N. E.; O'Keeffe, M. *Acta Crystallogr., Sect. B* **1991**, *47*, 192.

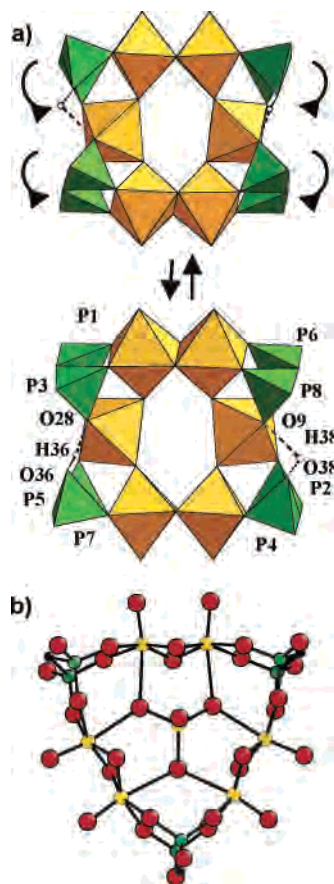


Figure 5. (a) Polyhedral representation of the anion in **3a**, common with the anion in **3d** (orange octahedra = MoO₆ and green tetrahedra = PO₃C). The arrows indicate the possible flip-flop motion of the PO₃ groups in solution. (b) Ball-and-stick representation of the anion in **3b**, present also in **3c**.

161.42(11)°] than the O38–H38···O9 one [H36···O28 = 2.26(1) Å; O36–H36···O28 = 101.60(12)°].

The anion in **3b** and **3c** has a triangular shape (Figure 5b), with one Mo^V dimer at each side and one methylenediphosphonato ligand at each corner of the anion. The center of the triangle is occupied by a Mo^{VI} tetrahedron. The anion has thus C_{3v} symmetry.

In **4a** and **4c**, the octanuclear wheel is reminiscent of the sulfite and carbonato wheels. The difference lies in the presence of two extra methylenediphosphonato ligands, related by an inversion center, inside the cavity (Figure 6a). Thus, the anion in **4a** and **4c** can be compared more precisely to the anti isomer in **2b** and **2d**, with one phosphonato group replacing one sulfite group. The common symmetry of these two anions is C_{2h}. Valence bond calculations (Table 2) have shown that among the three O atoms of the pending phosphate group one is protonated. In both structures, two Li⁺ ions occupy special positions inside the cavity of the wheels. Li1 and its symmetry-related ion are bound to four O atoms of three different methylenediphosphonato groups with a tetrahedral arrangement (Table 2 and Figure 6a). In **4a**, the two NH₄⁺ counterions are also located in the vicinity of the wheel (Figure 6b), and an intricate H-bonding scheme exists between the NH₄⁺ cations and the O atom of the wheel [H8···O6 = 2.02(1) Å, N1–H8···O6 = 167.0(5)°; H9···O8 = 2.04(1) Å, N1–H9···O8 = 158.0(5)°; H10···O21 =

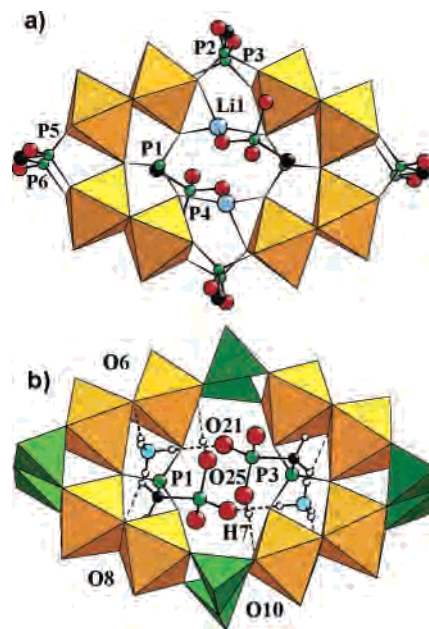


Figure 6. (a) Mixed ball-and-stick and polyhedral representation of the anion in **4a** common with the anion in **4c**, with the position of the two Li⁺ ions encapsulated in the wheel (orange octahedra = MoO₆, red sphere = O, green sphere = P, black sphere = C, and blue sphere = Li⁺). (b) Polyhedral representation of the anion in **4a**, with a H-bonding scheme between the O atom of the polyoxomolybdate core and the N atom of the NH₄⁺ counterion and the protonated pending phosphonato groups (cyan sphere = N).

Table 3. Computed and Observed Bond Lengths (Å, Averaged)^a for *syn*- and *anti*-[(Mo₂O₄)₄(O₃PCH₂PO₃)₄(SO₃)₂]¹²⁻

	<i>syn</i> (comp.)	2a (obs.)	<i>anti</i> (comp.)	2b (obs.)
Mo=O	1.736	1.686	1.736	1.680
Mo–O _{Mo}	1.971	1.949	1.970	1.936
Mo–O _P	2.112	2.095	2.114	2.084
Mo–O _i	2.30/2.52	2.336	2.31/2.50	2.368
P=O	1.525	1.513	1.525	1.498
P–O _{Mo}	1.576	1.542	1.576	1.544
P–C	1.826	1.802	1.826	1.796

^a All computed values resulting from an optimization with the COSMO solvent model.

1.99(1) Å, N1–H10···O21 = 178.7(5)°; Figure 6b] and between the protonated pending phosphonato group and one O atom of the wheel [H7···O10 = 1.84(1) Å, O25–H7···O10 = 163.4(5)°; Figure 6b].

DFT Calculations. Geometry optimizations carried out on the *syn* and *anti* forms of the [(Mo^V₂O₄)₄(O₃PCH₂PO₃)₄(SO₃)₂]¹²⁻ (**2**) anions using the continuum solvent model show that all interatomic bonding distances are correctly reproduced by calculation with a slight overestimation, comprised between 0.02 and 0.05 Å, attributable to the use of a generalized gradient approximation functional (Table 3). More importantly, all bonding distances are computed to be identical in the *syn* and *anti* conformations, indicating that the small bond-length variations observed between *syn*-**2a**, on the one hand, and *anti*-**2b** and **2d**, on the other hand, should be assigned to experimental uncertainties and/or to crystal forces. It also means that the energy difference computed between these two conformers should not be assigned an electronic origin but attributed either to intramolecular electrostatic or strain effects or to differences in

Table 4. Bond Energies (eV) and Relative Energies (kcal mol⁻¹) Calculated for the Isomers of Anion **2**, Assumed (i) Isolated and (ii) Embedded in a Continuum Solvent Model (COSMO Model) and for the {X₂-**2**} Host–Guest Complexes (X = Na⁺, NH₄⁺), in the Same Conditions

	bond energy (eV)		relative energy (kcal mol ⁻¹)	
	syn	anti	syn	anti
2	-445.3816	-445.4600	+1.81	0.0
2 + COSMO	-592.9145	-592.9941	+1.84	0.0
{Na ₂ - 2 }	-488.4336	-488.5246	+2.10	0.0
{(NH ₄) ₂ - 2 }	-528.4498	-528.5741	+2.87	0.0
{Na ₂ - 2 } + COSMO	-592.1705	-592.1561	0.0	+0.33
{(NH ₄) ₂ - 2 } + COSMO	-633.0191	-632.9804	0.0	+0.89

solvation energetics. Calculations show that **2**, assumed to be isolated, is slightly more stable in the anti form, with an energy difference of 1.8 kcal mol⁻¹. The trend and energy difference are not modified by the COSMO solvent model (Table 4). Attempts were then carried out to model the influence of the counterions by introducing into the polyoxoanion the two cations closest to the molecular cavity. All atoms in the syn and anti forms of the anionic cage were kept frozen at the position optimized for the free molecules, whereas the cations were positioned first at the places occupied by the water molecules O5W and O11W for the NH₄⁺ salt **2a** (Figure 4a) and by the Na⁺ ion Na3 in **2b** (Figure 4b) and then allowed to move along the frozen cage. Insertion of the counterions in the isolated anionic cages does not drastically modify the relative energies of the two isomers: the computed energy difference is comprised between 2 and 3 kcal mol⁻¹, still in favor of the anti form. Note that the Na⁺ counterions are slightly less favorable to the anti form than NH₄⁺ (Table 4). Finally, embedding the host–guest complex made from the anionic cage and the two cations into the continuum solvent model *reverses* the energy ordering of the two isomers: the syn form becomes slightly more stable with both types of counterions. The computed energy differences decrease below 1.0 kcal mol⁻¹, highlighting the extreme sensitivity of the equilibrium to environmental changes. It is now found that the Na⁺ counterions fit somewhat better to the anti form and reduce the computed energy gap from 0.9 to 0.3 kcal mol⁻¹ (Table 4), a trend that is in agreement with the observed conformational changes.

³¹P NMR Characterization of 1–4 in Aqueous Solutions. The symmetry of each anion, deduced from the crystallographic studies, and thus the number of ³¹P NMR expected resonances with the relative intensities are summarized in Table 5. The anion in **1a** possesses a pseudo mirror plane containing the carbonato ligands; therefore, the P atoms within the same methylenediphosphonato ligand (P1 and P2, P3 and P4; Figure 3a) are expected to be equivalent and noncoupled and, therefore, P1 and P2 should give one signal and P3 and P4 should give a signal of equal intensity. The spectrum of **1a** dissolved in water exhibits two resonances of equal relative intensity (Figure 7a), in agreement with these symmetry considerations. The attribution of the resonances is deduced from experiments showing the influence of the nature of the counterion on the chemical shifts of each resonance. For these experiments, **1a** is dissolved in

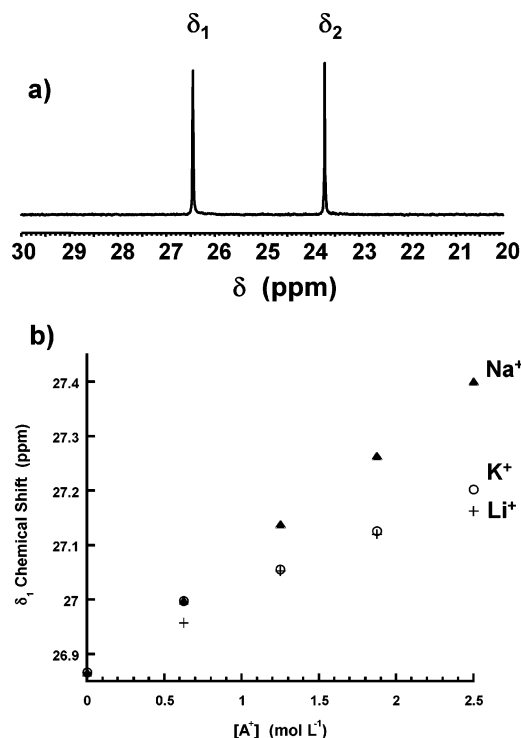





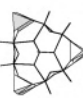



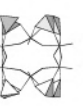
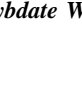
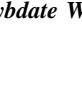


Figure 7. (a) ³¹P NMR spectrum of **1a** dissolved in water. (b) Dependence of the δ₁ relative intensity vs cation concentration.

mixtures of NH₄⁺Cl and ACl (A = Li⁺, Na⁺, K) solutions in order to keep the ionic strength constant. When the concentration of ACl increases, the δ₂ resonance is only very slightly affected, while δ₁ moves continuously toward low-field values (Figure 7b). With Na⁺ ions, the resonances are close to the one observed for a pure aqueous solution of **1b** (Table 5). On the basis of the structural characterization of **1a**, it can be expected that one alkali cation will interact directly with the anionic cavity to form an ion-pairing complex (Figure 3b). δ₁ is thus attributed to the methylenediphosphonato group closest to the alkali cation, i.e., P1 and P2 phosphorus atoms. The greater sensitivity of the δ₁ chemical shift toward the presence of Na⁺ ions shows that the anion has a greater affinity for Na⁺ than for K and Li⁺ ions and that the stability of the ion-pairing complex is increased in the order Li⁺ < K⁺ < Na⁺. The ³¹P NMR spectrum of the synthetic solution of **1c** exhibits two peaks with chemical shifts intermediate between those of **1a** and **1b** (Table 5), showing that this compound is formed quantitatively in solution.

³¹P NMR spectroscopy shows that **2a** and **2b** decompose in a pure aqueous solution but can be stabilized by the presence of sulfite ions. The ³¹P NMR spectrum of a solution of **2a** in ammonium sulfite (Figure 8a) exhibits two doublet of doublets corresponding to an AB system of an asymmetrical methylenediphosphonato group, in agreement with the pseudo C_{2h} symmetry of the syn isomer. By analogy with the ³¹P NMR study of **1a**, the four lines at 26.48, 26.35, 26.00, and 25.87 ppm are assigned to the P atoms labeled P1 and P2 in Figure 4a, which are equivalent to P5 and P6, a consequence of the presence of a pseudo mirror plane containing the two sulfite ions. Similarly, the four lines at

Table 5. Idealized Symmetry, Schematic Drawing of the Anions, and ^{31}P NMR Chemical Shifts in **1–4**

Compound	1a	2a	3a	4a	1b	2b	3b	1c	3c	4c	2d	3d
Idealized symmetry of the anion	D_{2h}	C_{2v}	C_s	C_{2h}	D_{2h}	C_{2h}	C_{3v}	D_{2h}	C_{3v}	C_{2h}	C_{2h}	C_s
Representation												
Counter-ion	12 NH_4^+	12 NH_4^+	10 NH_4^+	2 NH_4^+ 12 Li^+	12 Na^+	12 Na^+	8 Na^+	12 Li^+	8 Li^+	14 Li^+	1 Na^+ 11 NH_4^+	9 Li^+ Cl^- , 9 Li^+ 2 NH_4^+
Expected ^{31}P NMR peaks	2	8	8	9	2	5	4	2	4	9	8	8
Expected relative intensities	1:1	1:1:1:1	1:1:1:1	1:1:4:1:1	1:1	4:1:1:1:1	1:1:1:1	1:1	1:1:1:1	1:1:4:1:1	1:1:1:1	1:1:1:1
Solvent	H_2O	0.5 M $(\text{NH}_4)_2\text{SO}_3$	H_2O	H_2O	H_2O	0.5 M Na_2SO_3	H_2O	synthetic solution	H_2O	H_2O	0.5 M $(\text{NH}_4)_2\text{SO}_3$	H_2O
δ/ppm	26.43 23.69	26.48 26.35 25.87 25.85 23.99 23.85 23.37 23.23	22.99 22.88 21.64 21.53	29.95 29.88 27.10 24.16 24.02 23.28 23.14 19.79 19.71	27.30 23.95	26.88 26.76 (♦) ^a 26.69 26.56 24.03 23.99 (♦) 23.89 23.85 (♦) 23.64 (♦) 23.50 (♦) 23.46 23.32	25.46 25.33 24.68 24.55	27.03 23.86	25.28 25.14 24.19 24.05	29.68 29.60 27.10 24.20 24.06 23.32 23.18 20.16 20.08	26.90 26.77 26.43 26.30 24.42 24.28 23.80 23.66	24.02 22.91 21.67 21.56

^a The black diamonds refer to the anti isomer (Figure 4b).

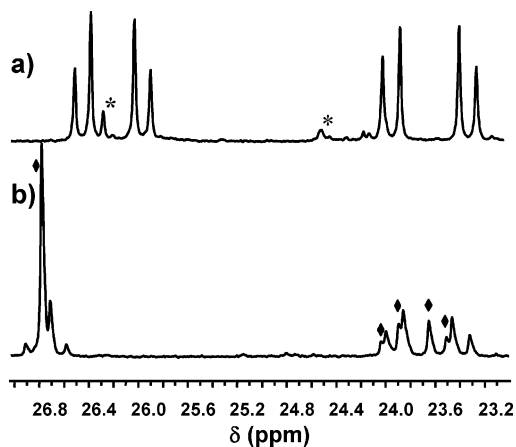


Figure 8. ^{31}P NMR spectra of a solution of (a) **2a** dissolved in 0.5 M $(\text{NH}_4)_2\text{SO}_3$, (* = unknown impurities) and (b) **2b** dissolved in 0.5 M Na_2SO_3 (◆ = anti isomer).

23.99, 23.85, 23.37, and 23.23 ppm are attributed to P3 and P4, equivalent to P7 and P8. The coupling constants $^2J_{\text{P-C-P}}$ between P1 and P2 (15.8 Hz) and P3 and P4 (17.0 Hz) deduced from the ^{31}P NMR spectrum are close to those observed for other methylenediphosphonate/POM systems.^{12c,13} The spectrum of a solution of **2b** in sodium sulfite is more complicated (Figure 8b) and can be interpreted by the presence of both the anti and syn isomers in solution. As mentioned above, the syn isomer is characterized by two doublet of doublets (peaks with no marks in Figure 8b, with one of the doublets being slightly unshielded compared to the spectrum of the syn isomer in ammonium sulfite solutions shown in Figure 8a), while the anti isomer is characterized by five resonances (peaks marked with black diamonds in Figure 8b): a single peak attributed to the four equivalent P atoms P1, P2, P1*, and P2* (Figure 4b) and a doublet of doublets ($J = 17.0$ Hz) assigned to P3, P4, P3*, and P4*. The integration of the peaks allows an estimation of the proportion of each isomer: around 64% of the anti isomer and 36% of the syn isomer. To study the influence of the composition of the solution on the proportion of each isomer, ^{31}P NMR spectra of a solution of **2b** dissolved in aqueous sodium sulfite/ammonium sulfite solutions have been recorded. Selected spectra are shown in Figure 9a. When the proportion of NH_4^+ cations increases, the relative intensity of the peaks attributed to the syn isomer increases continuously (Figure 9b). The proportion of the syn isomer thus reaches a value of around 70% in a pure NH_4^+ solution. This study shows that an equilibrium between the anti and syn forms exists in solution and that the proportion of each isomer depends on the nature of the cations (NH_4^+ or Na^+). Contrary to what is observed in the solid state (see above), in solution the presence of Na^+ ions in the medium is not a determining factor for the stabilization of the anti isomer. On the other hand, the syn isomer seems to be stable in pure NH_4^+ solutions. Another experimental proof of these assumptions is the fact that the ^{31}P NMR spectrum of **2d** dissolved in 0.5 M $(\text{NH}_4)_2\text{SO}_3$ only exhibits the peaks of the syn isomer (Table 5). This means that the Na^+ ion present in the cavity of the ring in the solid state, stabilizing the anti isomer, is replaced by NH_4^+ ions of the medium.

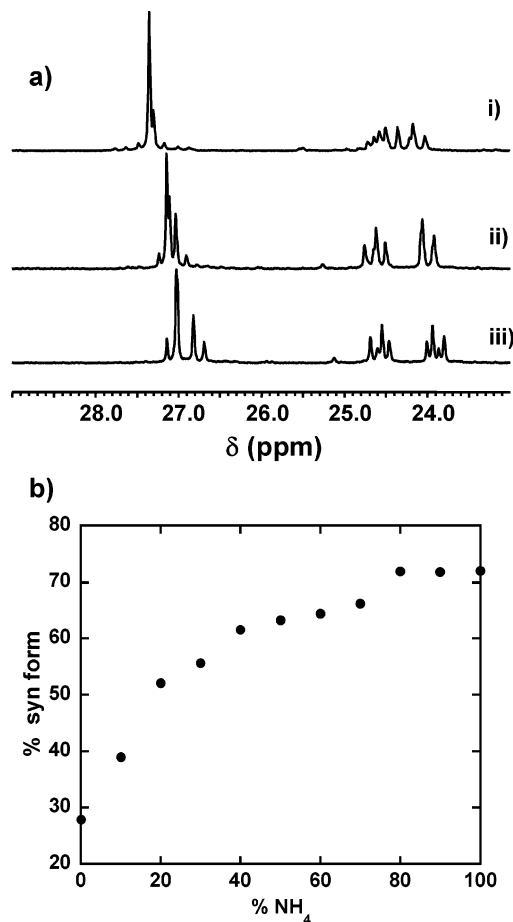


Figure 9. (a) Changes of the ^{31}P NMR spectrum of a solution of **2b** dissolved in mixtures of 1 M Na_2SO_3 and 1 M $(\text{NH}_4)_2\text{SO}_3$ with the proportion of NH_4^+ ions: (i) pure 1 M Na_2SO_3 aqueous solution; (ii) 1:1 1 M Na_2SO_3 /1 M $(\text{NH}_4)_2\text{SO}_3$; (iii) pure 1 M $(\text{NH}_4)_2\text{SO}_3$ aqueous solution. (b) Evolution of the proportion of the syn form of the anion in **2a**.

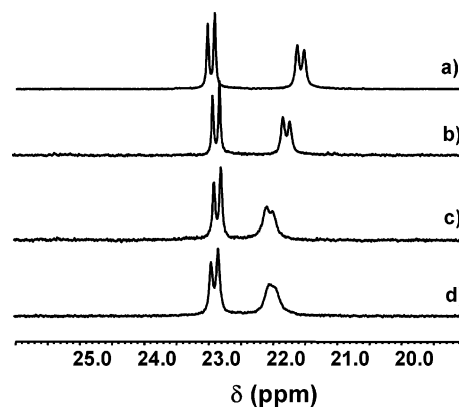


Figure 10. ^{31}P NMR spectra of a solution of **3a** dissolved in (a) H_2O , (b) 6 M LiCl , (c) 1:1 6 M LiCl /6 M NaNO_3 , and (d) 6 M NaNO_3 .

The ^{31}P NMR spectrum of a solution of **3a** in a pure water solution (Figure 10a) exhibits only one doublet of doublets although two should be expected from the C_s symmetry of the anion. The presence of only one doublet indicates that the four methylenediphosphonate ligands are equivalent in solution; i.e., one doublet is attributed to P1, P2, P5, and P6 (Figure 5a) and the other one to P3, P4, P7, and P8. The shape of the doublet at high field depends on the nature of the solution; indeed, the spectrum of **3a** in LiCl is similar to

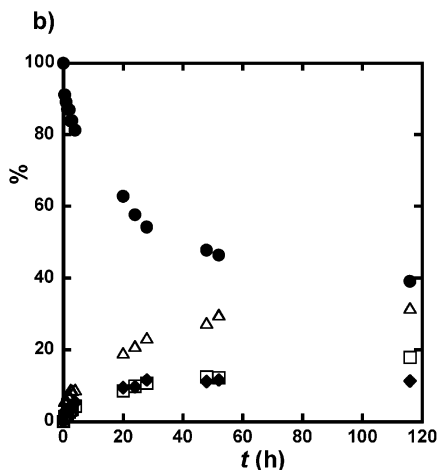
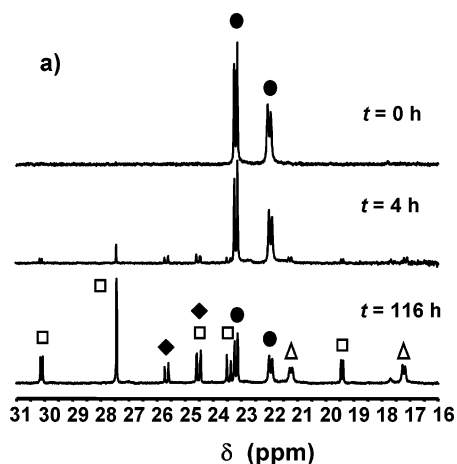


Figure 11. Changes with time (a) of the ^{31}P NMR spectrum of a solution of **3a** in 3 M LiCl heated at 45 °C and (b) of the proportion of each species deduced by the integration of the peaks: (□) anion of **4a**; (◆) anion of **3c**; (●) anion of **3a**; (△) unknown species.

the spectrum of **3a** in water, while a coalescence of the doublet at high field is observed in NaNO_3 or NaCl solutions (Figure 10). The equivalence of P3, P4, P7, and P8 and the line broadening are characteristic of dynamic behavior and are attributed to a flip-flop motion of the four P3, P4, P7, and P8 phosphonato groups as shown by the arrows in Figure 5a. This flip-flop motion involves the breaking of one Mo–O(PO₂C) bond and the formation of another with a concomitant move of one proton from one P–O bond to the other, probably favored by the H-bond interaction between both O atoms. The four P3, P4, P7, and P8 atoms thus become equivalent and are characterized by the doublet at high field. The presence of Na⁺ cations seems to facilitate this dynamic exchange.

The evolution of a solution of **3a** in LiCl heated at 45 °C has been followed by ^{31}P NMR spectroscopy. A few representative spectra in the 0–116-h range are shown in Figure 11a. After 4 h, several new additional resonances are observed, attributed to three different species. The ^{31}P NMR spectrum (Table 5) of the recrystallization product of **3a** in LiCl, **4a**, allows the attribution of a series of peaks (labeled with squares). The doublet of doublets marked with a black diamond is assigned to the hexanuclear anion common in **3b** and **3c**. The remaining doublets of doublets marked with

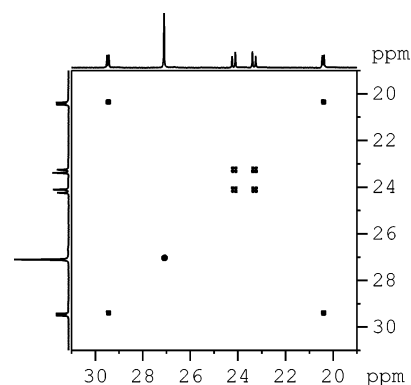


Figure 12. Contour plot of a two-dimensional COSY ^{31}P NMR experiment for **4c**. The mixing time was 100 ms.

triangles correspond to species so far unknown in this family. This species, which contains one or more asymmetric equivalent methylenediphosphonato ligands, could be the tetranuclear complex evidenced by Chang and Zubietta¹⁴ although, as discussed in the Introduction, in this anion the connecting mode of the methylenediphosphonato ligands to the Mo^V dimers is different from what is observed in the complexes described here (Figure 1). While the amount of **3a** decreases, the proportions of each species formed increase continuously with time (Figure 11b) in the 0–60-h range and seem to reach a plateau after 116 h. Only 20% of the anion of **3a** is converted into the anion of **4a**, a result consistent with the poor yield observed for the recrystallization. It should be noted that the spectrum of a solution of **3a** heated at 60 °C for 116 h in pure water or in 1 M NaCl exhibits only the peaks attributed to the hexanuclear anion common in **3b** and **3c** and to the unknown species. The peaks of the octanuclear anion common in **4a** and **4c** could not be detected. Furthermore, the proportion of the initial species **3a** is around 80% in pure water or a 1 M NaCl solution, while it is around 40% in 1 M LiCl. Therefore, the presence of Li⁺ ions in the solution seems essential for the formation of the octanuclear anion and strongly increases the degradation of **3a**.

The spectrum of **4c** exhibits four doublets of equal intensity and a singlet at 27.10 ppm, the relative intensity of which is equal to double that of a doublet. The first components of the first AB system are at 29.68 and 29.60 ppm and the second at 20.16 and 20.08 ppm, while the lines at 24.19, 24.06, 23.32, and 23.18 ppm correspond to the second AB system. To confirm this assumption, a two-dimensional COSY ^{31}P NMR experiment was carried out (Figure 12) and clearly shows that the lines at 29.68 and 29.60 ppm and 20.16 and 20.08 ppm as well as the lines at 24.19 and 24.06 ppm and 23.32 and 23.18 ppm are respectively correlated by four off-diagonal spots. They can therefore be assigned to two different asymmetrical methylenediphosphonato ligands. The doublet at 20.16 and 20.08 ppm is attributed to the P atoms of the pending phosphonato groups (labeled P4 in Figure 6a) because these peaks are the most shielded peaks and have chemical shift values closer to uncoordinated methylenediphosphonato ligands (16.9 ppm). The other component of the AB system at 29.68 and

29.60 ppm corresponds to the phosphonato group encapsulated within the wheel (labeled P1 in Figure 6a). The second doublet of doublets is assigned to P5 and P6, while the single peak at 27.10 ppm is attributed to P3 and P4, in comparison with the spectrum of the anti isomer in **2b**. The coupling constant ${}^2J_{\text{P1-C-P4}}$ (9.7 Hz) is smaller than the ${}^2J_{\text{P5-C-P6}}$ constant (17.0 Hz), which is more on the order of those observed previously for ligands within the octa- and hexanuclear wheels of this family of anions (see above). In oxothiomolybdate wheels containing pyrophosphate groups, the ${}^2J_{\text{P-O-P}}$ constant has been correlated to the P–O–P angle, with larger coupling constants arising from larger P–O–P angles.²³ A similar correlation does not seem possible for the methylenediphosphonato ligand. Indeed, the P1–C–P4 [118.3(3)°] and P5–C–P6 [111.6(3)°] angles determined in the structure of **4c** are close and cannot explain the difference between the coupling constants. It can tentatively be supposed that in solution the P1–C–P4 angle is lowered.

Conclusion

In conclusion, the acid–base condensation of the $[\text{Mo}^{\text{V}}_2\text{O}_4(\text{H}_2\text{O})_6]^{2+}$ oxocation with $[\text{O}_3\text{PCH}_2\text{PO}_3]^{4-}$ ligands has afforded a large diversity of compounds showing the versatility of this system. We have shown that small inorganic or organic ligands (SO_3^{2-} , CO_3^{2-} , $\text{O}_3\text{PCH}_2\text{PO}_3^{4-}$) can be encapsulated within the octanuclear Mo^{V} framework $\{(\text{Mo}^{\text{V}}_2\text{O}_4)_4-$

$(\text{O}_3\text{PCH}_2\text{PO}_3)_4\}$. With MoO_4^{2-} , two different hexanuclear anions have been isolated. It should be noted that, with CH_3CO_2^- or HCO_2^- ligands, it had not been possible to characterize any product with Li^+ and NH_4^+ counterions although double-wheel-shaped anions had been previously synthesized with Na^+ counterions.¹³ On the contrary, with CO_3^{2-} , the same octanuclear wheel is formed, whatever the counterion (NH_4^+ , Na^+ , and Li^+). Besides this unique case, this study has evidenced the crucial role of the counterions in the structure and stability of the Mo^{V} complexes. Such a family is of great interest for ionic conductivity measurements. Indeed, by analogy with previous results from our group on Li^+ and Na^+ salts of oxothiomolybdate rings,²⁴ these salts could exhibit good ionic (protonic or alkali) conducting properties. Furthermore, the functionalization of Mo^{V} can be envisioned by the use of R-SO_3^- , R-PO_3^{2-} , or R-AsO_3^{2-} (R = organic group) as an exogeneous ligand.

Acknowledgment. A.D. thanks Jean-Daniel Compain, a student from ENS Lyon, for his contribution to the synthesis and ${}^{31}\text{P}$ NMR study of these compounds and Marie-José Pouet and Chantal Robert-Labarre for their help concerning the NMR studies.

Supporting Information Available: X-ray crystallographic data (CIF files). This material is available free of charge via the Internet at <http://pubs.acs.org>.

IC060410+

(23) Cadot, E.; Pouet, M.-J.; Robert-Labarre, C.; du Peloux, C.; Marrot, J.; Sécheresse, F. *J. Am. Chem. Soc.* **2004**, *126*, 9127.

(24) du Peloux, C.; Dolbecq, A.; Barboux, P.; Laurent, G.; Marrot, J.; Sécheresse, F. *Chem.—Eur. J.* **2004**, *10*, 3026.